Electronic Supplementary Information

Toward a universal polymeric material for electrode buffer layers in organic and perovskite solar cells and organic light-emitting diodes

Qiang Zhang,[†a] Wei-Ting Wang,[†b] Cheng-Yu Chi,[b] Tobias Wächter,[c] Jhih-Wei Chen,[d] Chou-Yi Tsai,[a] Ying-Chi Huang,[a] Michael Zharnikov*[c] Yian Tai*[b] and Der-Jang Liaw*[a]

[a] Polymer Science and Materials Lab., Department of Chemical Engineering, National Taiwan University of Science and Technology, Taipei 10607, Taiwan.

[b] Nanohybrid Materials and Devices Lab., Department of Chemical Engineering, National Taiwan University of Science and Technology, Taipei 10607, Taiwan.

[c] Applied Physical Chemistry, Heidelberg University, Heidelberg 69120, Germany.

[d] Department of Physics, National Cheng Kung University, Tainan 70101, Taiwan.

*Corresponding authors:

Prof. Michael Zharnikov

Email: Michael.Zharnikov@urz.uni-heidelberg.de

Prof. Yian Tai

E-mail: ytai@mail.ntust.edu.tw; Tel: +886-2-2737-6620

Prof. Der-Jang Liaw

E-mail: liawdj@mail.ntust.edu.tw; liawdj@gmail.com; Tel: +886-2-2737-6638

† Q. Zhang and W.-T. Wang contributed equally to this work.

Materials

The chemicals, 4-isopropylbenzenamine (TCI, 98%), 2-(dimethylamino)ethanol (Aldrich, 98%), 1-bromo-4-iodobenzene (Acros, 98%), 1,1'-bis(diphenylphosphino)ferrocene (DPPF; Acros, 98%), 2-isopropoxy-4,4,5,5-tetramethyl-1,3,2-dioxaborolane (Aldrich, 98%), *n*-butyllithium (Acros, 2.5 M in hexanes), thionyl chloride (Aldrich, 97%), sodium *tert*-butoxide (Acros, 98%), tetrakis(triphenylphosphine)palladium(0) ($Pd(PPh_3)_4$) (Acros, 99%), bis(dibenzylideneacetone)palladium(0) ($Pd(dba)_2$) (Acros, 96%) and anhydrous potassium carbonate (Fisher Scientific, ≥99%) were purchased and used as received from commercial sources. Tetrahydrofuran was purchased from Merck, and toluene was dried and distilled over sodium metal under inert nitrogen atmosphere. The reagents 4-hydroxy-*N,N*-bis(4-bromophenyl)aniline[1] and 2-dimethylaminoethylchloride hydrochloride[2] were synthesized according to previously reported procedures. The polyfluorene (PFO) was prepared according to a well-known procedure[3]. PEDOT:PSS (AL 4083) was purchased from Clevios. P3HT (Mn: 36K) was purchased from Rieke Metals, Inc. $PC_{61}BM$ was purchased from Solenne BV. 1,8-Diiodooctane (DIO) and lead (II) iodide (99.9985%) was purchased from Alfa Aesar. Hydriodic acid (55%) and methylamine (40%) was purchased from TCI. $SnCl_2 \cdot 2H_2O$ was purchased from Merck. The acetic acid and ethyl acetate were purchased from Acros.

Synthetic route of PDTON

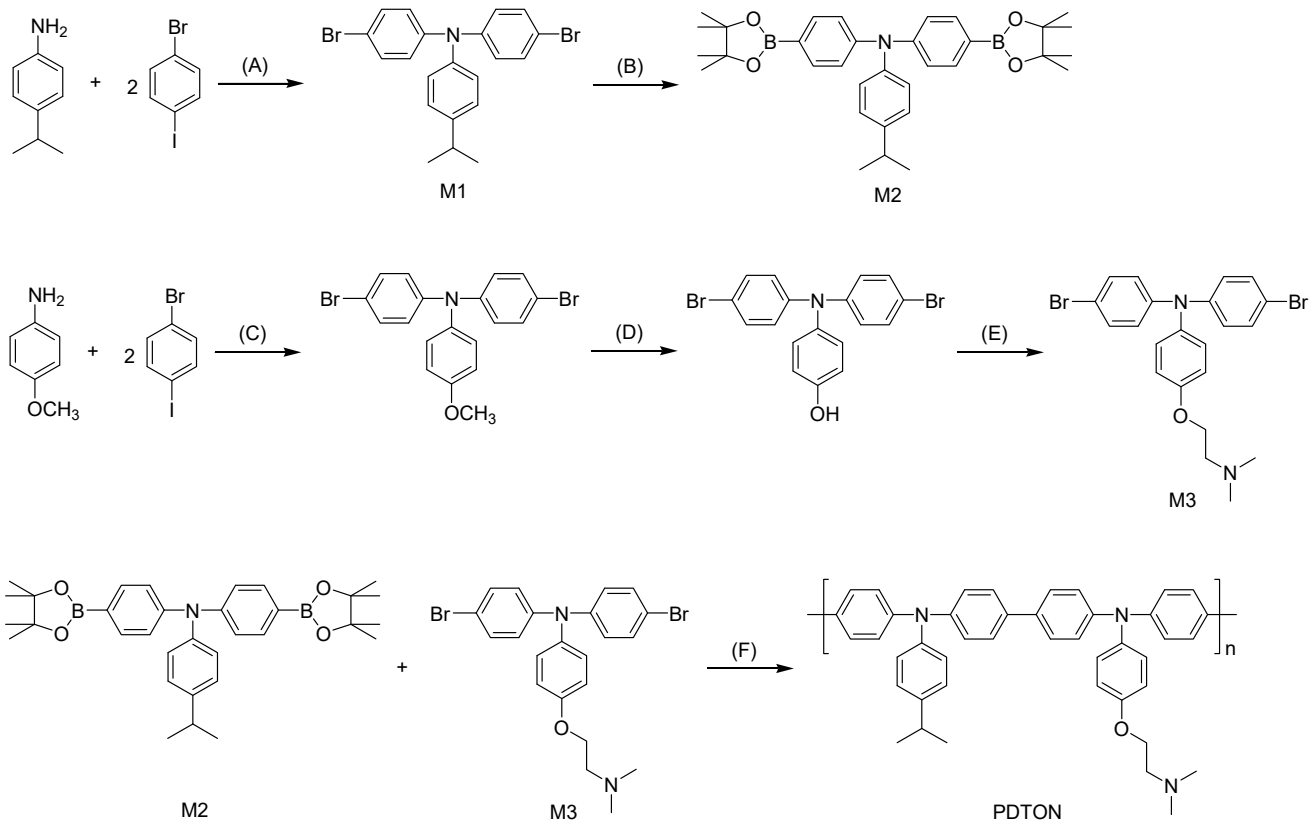

Scheme S1 Synthetic routes of PDTON. (**A**) $Pd(dba)_2$, DPPF, sodium *tert*-butoxide, toluene, 110 °C, 12 h; (**B**) i) *n*-BuLi, THF, -78 °C, 30 min ii) 2-isopropoxy-4,4,5,5-tetramethyl-1,3,2-dioxaborolane, THF, -78 °C, 2 h; (**C**) and (**D**) were described according to the literature;[1] (**E**) 2-dimethylaminoethylchloride hydrochloride, acetone, K_2CO_3, 80°C, 6 h; (**F**) $Pd(PPh_3)_4$, K_2CO_3, toluene, H_2O, 105 °C, 8 h.

Monomer Synthesis

Synthesis of Monomer M1

N,N-bis(4-bromophenyl)-4-isopropylbenzenamine (M1) was synthesized by the Buchwald–Hartwig reaction from 4-isopropylbenzenamine and 1-bromo-4-iodobenzene. A three-necked flask under inert nitrogen atmosphere was charged with 4-isopropylbenzenamine (1.45 g, 10.74 mmol), 1-bromo-4-iodobenzene (6.08 g, 21.48 mmol), $Pd(dba)_2$ (123.5 mg, 2.15×10^{-1} mmol), DPPF (237.9 mg, 4.30×10^{-1} mmol), sodium *tert*-butoxide (3.10 g, 32.21 mmol), and 20 ml of dry toluene, the reaction was heated to reflux for 12 h with stirring. After reaction completion, solvent was removed by vacuum. The solid residue was extracted with

dichloromethane and water, and the organic layer was collected and dried over anhydrous $MgSO_4$ overnight, followed by filtration to remove the drying agent. Dichloromethane solvent was removed under vacuum and the resultant residue was purified by column chromatography (silica gel, hexane) to obtain *N,N*-bis(4-bromophenyl)-4-isopropylbenzenamine as a colorless viscous liquid (85% yield, 4.06 g). ν/cm (KBr) 3028 (Ar-H stretch), 2928, 2957, 2870 (C-C), 1580, 1483, 1510 (C=C), 1310 (Ar-N) and 1072, 1007 (Ar-Br). ^{1}H NMR (600 MHz, $CDCl_3$, Me_4Si) δ_H (ppm): 7.33 (m, 4H, H_f), 7.14 (m, 2H, H_c), 7.00 (m, 2H, H_d), 6.94 (m, 4H, H_e), 2.89 (sep, J = 7.2, 1H, H_b), 1.27 (d, J = 7.2, 6H, H_a). ^{13}C NMR (150 MHz, $CDCl_3$, Me_4Si) δ_C (ppm): 146.7 (C_{10}), 144.73 (C_7), 144.42 (C_8), 132.21 (C_9), 127.49 (C_3), 125.01 (C_5), 124.92 (C_4), 114.98 (C_6), 33.51 (C_2), 23.98 (C_1). ELEM. ANAL. Calcd. for $C_{21}H_{19}Br_2N$: C, 56.66%; H, 4.30%; Br, 35.90%; N, 3.15%. Found: C, 57.99%; H, 4.43%; N, 3.12%. m/z: 442.9879

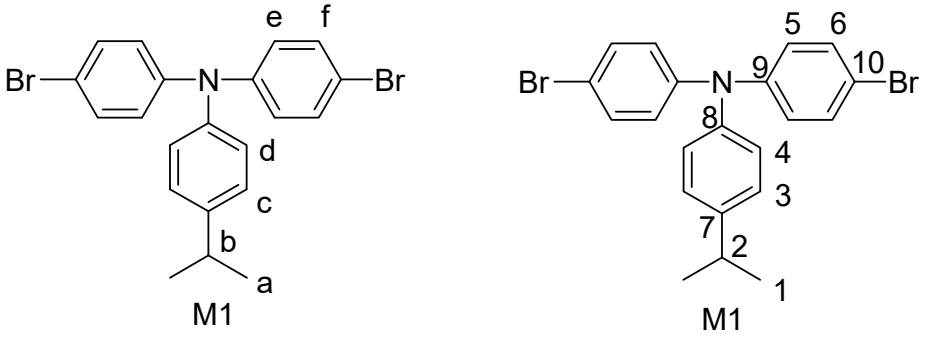

Fig. S1 Chemical structure of M1.

Synthesis of Monomer M2

4-isopropyl-*N,N*-bis(4-(4,4,5,5-tetramethyl-1,3,2-dioxaborolan-2-yl)phenyl)benzenamine (M2) was prepared from monomer M1. A three-necked flask under nitrogen atmosphere was charged with a solution of *N,N*-bis(4-bromophenyl)-4-isopropylbenzenamine (M1) (9.1 g, 20.44 mmol) in 130 ml of tetrahydrofuran. *n*-BuLi (20 ml of 2.5 M solution in hexanes, 50 mmol) was added dropwise to the flask, and the reaction mixture was stirred at -78 °C for 1 h, after which 2-isopropoxy-4,4,5,5-tetramethyl-1,3,2-dioxaborolane (25 ml, 123.24 mmol) was injected into the flask. The reaction mixture was stirred at -78 °C for 2 h and then equilibrated gradually to room temperature and stirred overnight. The product was precipitated in water and extracted with diethyl ether. The organic layer was collected, the diethyl ether was evaporated, and then the

solid residue was washed with water and dried. After filtration to remove $MgSO_4$ and subsequent solvent evaporation, the residue was recrystallized from hexane to give product M2 as a white solid (34% yield, 4.6 g). ν/cm (KBr) 3034 (Ar-H stretch), 2926, 2978, 2961, 2866 (C-C), 1595, 1510 (C=C), 1358 (Ar-N), 1319 (C-O), and 1090, 1140 (Ar-B). ^{1}H NMR (600 MHz, $CDCl_3$, Me_4Si) δ_H (ppm): 7.70 (d, J = 8.4, 4H, H_f), 7.15 (d, J = 8.4, 2H, H_c), 7.08 (d, J = 8.4, 4H, H_e), 7.05 (d, J = 8.4, 2H, H_d), 2.91 (sep, J = 7.2, 1H, H_b), 1.36 (s, 24H, H_g), 1.28 (d, J = 7.2, 6H, H_a). ^{13}C NMR (150 MHz, $CDCl_3$, Me_4Si) δ_C (ppm): 150.25 (C_{11}), 144.72 (C_8), 144.52 (C_9), 135.81 (C_7, C_{10}), 127.3 (C_4), 125.69 (C_5), 122.42 (C_6), 83.54 (C_{12}), 33.5 (C_3), 24.84 (C_1), 23.98 (C_2). ELEM. ANAL. Calcd. for $C_{33}H_{43}B_2NO_4$: C, 73.49%; H, 8.04%; B, 4.01%; N, 2.60%. Found: C, 73.35%; H, 8.78%; N, 2.13%. m/z: 527.844.

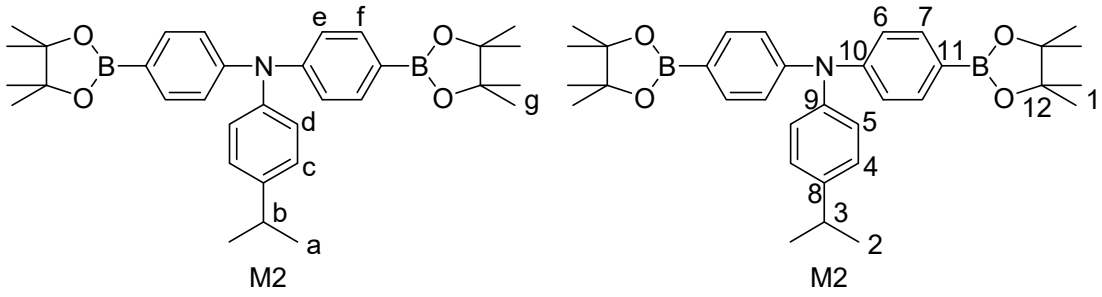

Fig. S2 Chemical structure of M2.

Synthesis of Monomer M3

A three-necked flask under inert nitrogen atmosphere was charged with anhydrous potassium carbonate (2.76 g, 20 mmol), 2-dimethylaminoethylchloride hydrochloride (1.73 g, 12 mmol), and 4-hydroxy-*N,N*-bis(4-bromophenyl)aniline (3.35 g, 8 mmol) in 100 ml of dry acetone. Reaction mixture was stirred at reflux for 6 h and subsequently precipitated in 200 ml of distilled water. The reaction mixture was extracted in two portions with 100 ml of ether for each extraction. The organic phase was collected and washed with H_2O (160 ml) and dried over $MgSO_4$. The solvent was evaporated and the product was further purified by column chromatography (alumina oxide, ether: triethylamine = 25:1) to give product M3 as a colorless viscous liquid (3.4 g, 79%). ν/cm (KBr) 3038 (Ar-H stretch), 2940, 2818, 2968, 2862 (C-C), 1580, 1483, 1503 (C=C), 1312 (Ar-N), 1281 (C-N), 1238, 1030 (C-O), and 1070, 1005 (Ar-Br). ^{1}H NMR (600 MHz, $CDCl_3$, Me_4Si) δ_H (ppm): 7.30 (d, 4H, H_g), 7.02 (d, 2H, H_d), 6.88 (d, 4H, H_f), 6.86 (d, 2H, H_e), 4.06 (t,

J = 5.7, 2H, H_c), 2.75 (t, J = 6.0, 2H, H_b), 2.36 (s, 6H, H_a). ^{13}C NMR (150 MHz, $CDCl_3$, Me_4Si) δ_C (ppm): 155.92 (C_8), 146.75 (C_{10}), 139.74 (C_9), 132.11 (C_7), 127.258(C_4), 124.25 (C_6), 115.63 (C_5), 114.51 (C_{11}), 66.2 (C_3), 58.24 (C_2), 45.84 (C_1). ELEM. ANAL. Calcd. for $C_{22}H_{22}Br_2N_2O$: C, 53.90%; H, 4.52%; Br, 32.60%; N, 5.71%. Found: C, 53.94%; H, 4.56%; N, 5.72%. m/z: 489.0172.

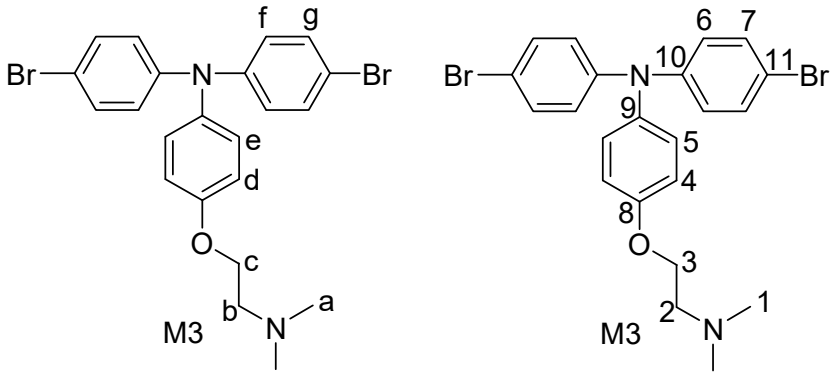

Fig. S3 Chemical structure of M3.

Polymer Synthesis

Synthesis of the Conjugated Polymer PDTON

Poly[N-(4-isopropylphenyl)-4,4'-diphenylamine-*alt*-*N*-(*p*-(*N,N*-dimethylamino))phenyl-4,4'-diphenylamine] (PDTON) was synthesized by Suzuki Coupling from monomers M2 and M3. A three-necked flask thoroughly evacuated and filled with nitrogen gas was charged with 4-isopropyl-*N,N*-bis(4-(4,4,5,5-tetramethyl-1,3,2-dioxaborolan-2-yl)phenyl)benzenamine (M2) (0.539 g, 1.1 mmol), 4-(*N,N*-dimethylamino)ethoxy-*N,N*-bis(4-bromophenyl)aniline (M3) (0.490 g, 1.1 mmol), and 7 ml of degassed toluene. After monomers dissolution, tetrakis(triphenylphosphine)palladium(0) $Pd(PPh_3)_4$ (23 mg, 0.2 mmol) and sodium carbonate aqueous solution (7 ml, 3M) were added to the flask. The mixture was stirred at 105 °C for 8 h under inert nitrogen atmosphere. After reaction completion, the reaction mixture was gradually cooled to room temperature. The organic layer was collected, extracted with water and precipitated in methanol. The precipitate was gravity filtered, extracted using toluene : H_2O (200 mL : 200 mL) for three times. The extraction procedure generated significant emulsification, with most of the emulsified part being removed to get the resulting product as clean as possible. The resulting toluene

solution was concentrated and precipitated in methanol, and subsequently dried, followed by Soxhlet extraction with methanol for 48 h to obtain product PDTON as a light yellow powder (14% yield, 0.1 g). In addition, the emulsified part removed during the extraction processes could be dissolved in THF and repurified again, the yield of PDTON could be raised up to 32%. ν/cm (KBr) 3028 (Ar-H stretch), 2924, 2862, 2853, 2818 (C-C), 1601, 1505, 1491 (C=C), 1317 (Ar-N), 1261 (C-N), and 1238, 1030 (C-O). ^{1}H NMR (600 MHz, $CDCl_3$, Me_4Si) δ_H (ppm): 7.44 (8H, H_f and H_g), 7.14 (8H, H_e and H_h),7.12 (2H, H_i), 7.11 (4H, H_c and H_d), 6.89 (2H, H_j), 4.08 (2H, H_k), 2.90 (1H, H_b), 2.76 (2H, H_l), 2.37 (6H, H_m), 1.27 (6H, H_a). ^{13}C NMR (150 MHz, $CDCl_3$, Me_4Si) δ_C (ppm): 155.53 (C_{19}), 146.83 (C_{14}), 146.68 (C_{17}), 145.14 (C_{13}), 143.84 (C_{12}), 140.58 (C_{18}), 134.52 (C_{15}), 134.13 (C_{16}), 127.23 (C_{10}), 127.16 (C_9&C_{20}), 124.76 (C_7), 123.82 (C_8&C_{21}), 123.05 (C_6), 115.47 (C_{11}). ELEM. ANAL. Calcd. for $C_{43}H_{41}N_3O$: C, 83.87%; H, 6.71%; N, 6.82%. Found: C, 78.00%; H, 5.80%; N, 6.90%.

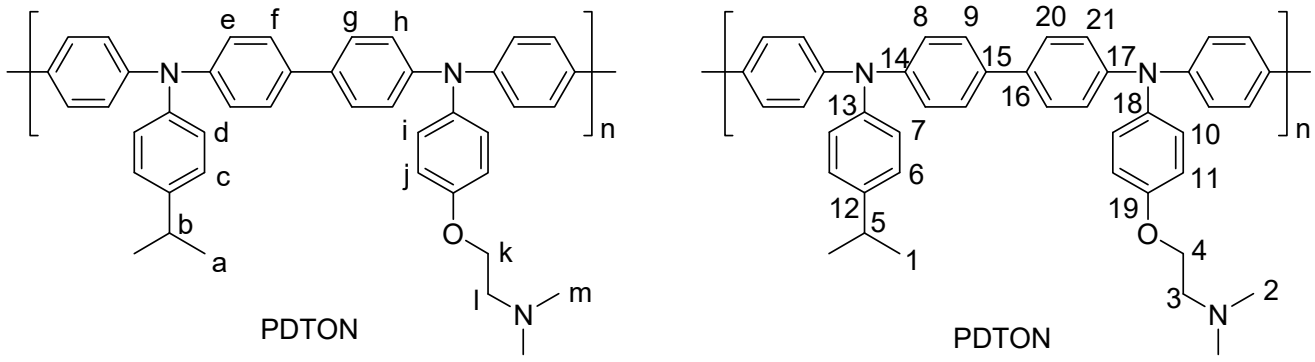

Fig. S4 Chemical structure of PDTON.

Thermal properties and molecular weight

The thermal properties of polymer were investigated by differential scanning calorimetry analysis (DSC) and thermogravimetric analysis (TGA) at a heating rate of 10 °C/min. The T_g of the PDTON was 169 °C. The TGA spectra of the PDTON showed no weight loss below 200 °C and 300 °C under air and nitrogen atmosphere, respectively. The decomposition temperatures at 10% weight loss (T_{d10}) and char yield at 800 °C were 434 °C and 60.5% in nitrogen, 368 °C and 12.8% in air, respectively. The molecular weight (Mn) of PDTON determined with gel permeation chromatography (GPC) was 8100 (PDI:1.3).

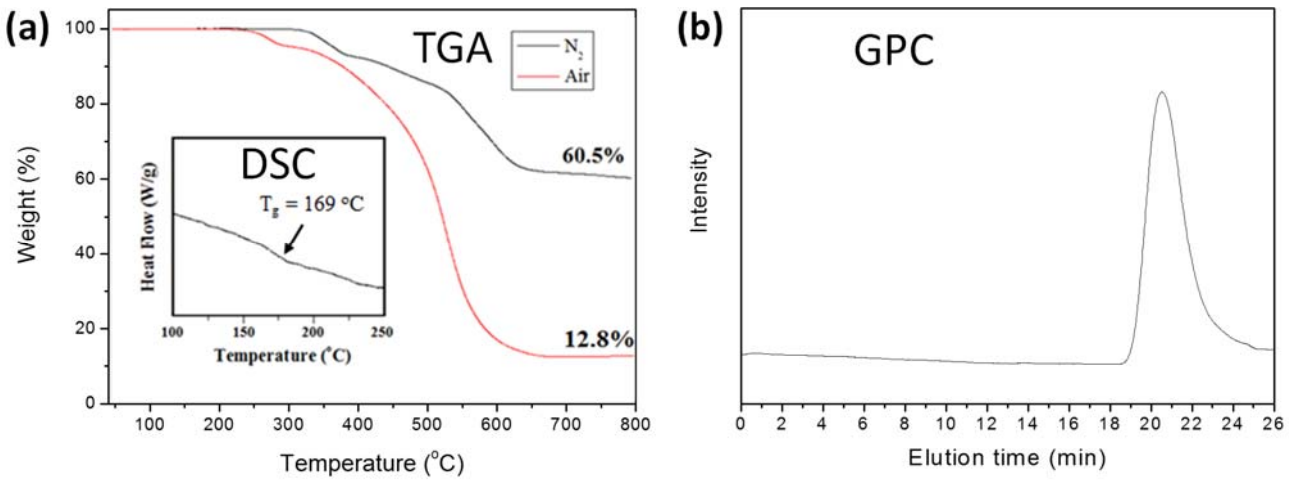

Fig. S5 (a) DSC and TGA of PDTON, (b) GPC of PDTON.

Methods

Polymer characterization and dispersion, device fabrication.

Polymer characterization. FT-IR spectrums were recorded in the range of 4000–400 cm^{-1} with a Bio-Rad FTS-3500 spectrometer. Elemental analysis was performed with Perkin-Elmer 2400 C, H, and N analyzer. The ^{1}H and ^{13}C NMR spectrums were recorded with a Bruker AVIII HD-600 instrument operating at 600 MHz for proton and 150 MHz for carbon. The glass transition temperature (T_g) was measured with a Du Pont 9000 differential scanning calorimeter (TA Instruments TA 910) at a heating rate of 10 °C min^{-1} from 50 to 250 °C under a steady flow of nitrogen. The glass transition temperature (T_g) was recorded on second run heating. The recorded temperatures were calibrated using indium as a standard. Thermogravimetric data were obtained with a Perkin-Elmer TG/DTA (Diamond TG/DTA). Experiments were carried out on approximately 5 mg sample at a heating rate of 10 °C min^{-1} from 50 to 800 °C under nitrogen or air flowing conditions (20 cm^3 min^{-1}). The molecular weight was measured with gel permeation chromatography (GPC) using a Waters Co. system (1515 HPLC pump, 2414 RI detector). The molecular weight (Daltons) of standard PMMA for GPC were 31,000, 14,700, 9680, 3480, 1750 and 904. UV-vis spectra of the polymer films were recorded with a JASCO V-670 spectrophotometer at room temperature in air. Photoluminescence

spectra were measured with a HORIBA Jobin Yvon FluoroMax-3 spectrofluorometer. Cyclic voltammetry (CV; CHI model 619A) was conducted with the use of a three electrode cell (composed of a 1 cm cuvette) in which ITO was used as a working electrode and a platinum wire was used as an auxiliary electrode at a scan rate of 50 mV/s against an Ag/Ag^+ reference electrode in a solution of 0.1 M tetrabutylammonium perchlorate (TBAP)/acetonitrile (CH_3CN). Water contact angle measurements were performed using CAM120 device from Creating Nano Technologies Inc. The thickness of the PDTON films were estimated using an absorbance-thickness curve[4] and SEM.

Preparation of the C-PDTON (PDTON55) solution. Two milligrams of PDTON were charged with nitrogen and then completely dissolved in 500 µl of acetic acid at 100 °C with stirring for 5 min. The mixture was cooled to room temperature, the acetic acid was evaporated under nitrogen flow until its residue was 55 mg, and then 1 ml of ethyl acetate was added and stirred for 15 min. Transparent yellow solution was obtained, which was then filtered by a 0.45 µm PVDF filter.

Preparation of the A-PDTON (PDTON15) solution. Two milligrams of PDTON were charged with nitrogen and then completely dissolved in 500 µl of acetic acid at 100 °C with stirring for 5 min. The mixture was cooled to room temperature, the acetic acid was evaporated under nitrogen flow until its residue was 15 mg, and then 1 ml of ethyl acetate was added and stirred for 15 min. An apparently turbid solution of PDTON was obtained and successively filtered by a 0.45 µm PVDF filter.

Preparation of the PDTON45, PDTON35, and PDTON25 solutions. Two milligrams of PDTON was charged with nitrogen and then completely dissolved in 500 µl of acetic acid at 100 °C with stirring for 5 min. The mixture was cooled to room temperature, the acetic acid was evaporated under nitrogen flow until its residue was 45 mg, 35 mg, or 25 mg and then 1 ml of ethyl acetate was added and stirred for 15 min. Solution of PDTON45, PDTON35, PDTON25 were obtained and successively filtered by 0.45 µm PVDF filters.

Fabrication and characterization of hole-only devices and electron-only devices. For the fabrication of hole-only devices, the patterned indium tin oxide (ITO) glass (sheet resistance = 15 Ω/□) was pre-cleaned in ultrasonic bath by deionized water, acetone, and isopropanol. After exposure to UV ozone for 10 min, the substrate was spin-coated with PEDOT:PSS solution at 3,000 rpm for 40 s and annealed at 150 °C for 10 min. Then the A-PDTON and C-PDTON solutions were spin-coated on the PEDOT:PSS film to form 30 nm films, annealed at 150 °C for 5 min. Then PEDOT:PSS was spin-coated on the A-PDTON and C-PDTON films respectively, annealed at 150 °C for 10 min, and then 100 nm of Ag were deposited to complete the hole-only device. For the fabrication of electron-only device, the pre-cleaned ITO substrate was spin-coated with ZnO nanoparticle solution[5] at 3000 rpm for 40 s. The ZnO film was annealed at 150 °C for 10 min, and then the A-PDTON and C-PDTON solutions were spin-coated onto the ZnO film to form 30 nm films each, annealed at 150°C for 5 min. Then ZnO nanoparticles were spin coated on the PDTON layer and annealed at 150 °C for 10 min, and, subsequently, 100 nm Al was deposited to complete the electron-only device. *J–V* characteristics of the electron-only device cells were measured using a Keithley 2400 source unit under ambient conditions. The hole and electron mobility of A- and C-PDTON were measured by using space charge limited current (SCLC) and fitting the results to the respective equation, $J = (8/9)\varepsilon_r\varepsilon_0\mu_e(V^2/L^3)$, where J is the current density; ε_r is the dielectric constant of conjugated polymer, which is assumed to be 3; ε_0 is the permittivity of free space; V is the voltage drop across the device; and the L is the thickness of the material. The configuration of a representative hole-only device was ITO/PEDOT:PSS/A- or C-PDTON/PEDOT:PSS/Ag, whereas the configuration of a representative electron-only device was ITO/ZnO/A- or C-PDTON/ZnO/Al.

Fabrication of inverted standard OPV. The pre-cleaned ITO substrate was spin-coated with sol-gel ZnO solution[6] at 6000 rpm for 40 s and annealed under ambient conditions at 150 °C for 10 min. The active layer was then deposited in a glove box by spin-coating of P3HT:$PC_{61}BM$ blend from a 1:0.8 wt. ratio solution in chlorobenzene with 3% vol. DIO at 1500 rpm for 45 s. The films were annealed at 130 °C for 20 min after

solvent annealing for 1 h in the glove box. Finally, 10 nm MoO_x and 100 nm Ag were subsequently thermally evaporated on the top of the cell at 10^{-5} Torr.

Fabrication of ABLD, CBLD, and CABLD. For the CBLD and CABLD configurations, the C-PDTON solution was spin-coated on top of the ITO substrate to form 10 nm film, annealed at 150 °C for 5 min. The P3HT:PC_{61}BM solution was then spin-coated at 1500 rpm for 45 s on top of the CBL. For the ABLD and CABLD configurations, the A-PDTON was deposited onto the P3HT:PC_{61}BM using a transfer technique[7] forming 20 nm film (A-PDTON layer could also be deposited by different fabrication processes, see Supplementary Fig. 16). For the CBLD, 10 nm of MoO_x were deposited onto the P3HT:PC_{61}BM. The device fabrication was completed by thermal evaporation of Ag as the anode under vacuum at a base pressure of 10^{-5} Torr.

Fabrication of OLEDs. Four devices included polyfluorene (PFO) sandwiched between ITO/PEDOT:PSS and the Al electrode (Supplementary Fig. 19a); ITO/PEDOT:PSS/PFO/C-PDTON/Al, with the C-PDTON film serving as CBL for electron injection (Supplementary Fig. 19b); ITO/A-PDTON/PEDOT:PSS/PFO/Al, with the A-PDTON film serving as ABL for hole injection (Supplementary Fig. 19c); and ITO/A-PDTON/PEDOT:PSS/PFO/C-PDTON/Al, with the A- and C-PDTON films serving as ABL and CBL, respectively (Supplementary Fig. 19d). The A-PDTON was spin-coated on top of the ITO substrate to form 20 nm film, annealed at 150 °C for 5 min. For the preparation of the A-PDTON/PEDOT:PSS bilayer ABL, the diluted PEDOT:PSS (0.43% in water, wt%) was directly spin-coated onto the A-PDTON film and annealed at 150 °C for 10 min. For the preparation of the PEDOT:PSS ABL, the PEDOT:PSS (1.3 % in water, wt%) was spin-coated onto the ITO substrate at 4000 rpm for 40 s and annealed at 150 °C for 10 min. 10 mg/ml PFO in chloroform was spin-coated onto the ABL. For the devices using C-PDTON as CBL, the C-PDTON was spin-coated onto PFO to form 5-10 nm film, annealed at 150 °C for 5 min. Finally, a 100 nm Al film was deposited through a shadow mask to form the cathode; the deposition was performed at a base pressure of 10^{-5} Torr. For the fabrication of the ITO/A-PDTON/PFO/C-PDTON/Al device, PFO was transferred onto A-PDTON using a transfer technique[7] to prevent dissolution of A-PDTON. All the

fabrication procedures except the deposition of Al electrode were conducted under ambient conditions with relative humidity of ~55%, and temperature of 25 °C.

Fabrication of conventional PSCs. The sol-gel ZnO layer of standard device was fabricated by the same procedures as in the case of the **Fabrication of inverted standard OPV**. For the preparation of the C-PDTON/ZnO CBL, the C-PDTON layer (thickness: 5-10 nm) was spin-coated onto the ITO substrate, dried for several minutes, then sol-gel ZnO was spin-coated onto the C-PDTON layer and annealed at 150 °C for 10 min. The standard device using sol-gel SnO_2 was fabricated as described.[8] For the preparation of the PDTON35/SnO_2 CBL, the PDTON35 layer (thickness: 5-10 nm) was spin-coated onto the ITO substrate and dried for several minutes, then sol-gel SnO_2 was spin-coated onto the PDTON35 layer and annealed at 190 °C for 2.5 h. The perovskite film was prepared according to a literature procedure.[5] Then, the spiro-OMeTAD was deposited onto the perovskite films by spin-coating of the respective solution (prepared according to a literature procedure[5]). The devices were completed by thermal evaporation of 100 nm Ag. The assembly was performed under ambient conditions (except the top electrode) with a relative humidity of ~55%, with temperature of 25 °C.

Fabrication of inverted PSCs. A-PDTON (20 nm, annealed at 150 °C for 5 min) and PEDOT:PSS were spin-coated onto the UV-ozone treated ITO substrates, respectively; the $CH_3NH_3PbI_3$ film was prepared according to a literature procedure.[5] The $PC_{61}BM$ (20 mg/ml in chlorobenzene) was spin-coated onto the perovskite film as CBL,[9] then 100 nm Ag were thermally deposited onto it. These devices were assembled under ambient conditions (except the top electrode) with a relative humidity of ~55%, with temperature of 25 °C.

OSC and PSC characterization. The device area was 0.04 cm^2. The *J–V* characteristics of the photovoltaic cells were measured using a Keithley 2400 source unit under a simulated AM 1.5G spectrum. A solar simulator (SS-F5-3A, Enli Technology Co., Ltd) was used, the light intensity was calibrated by a SRC-2020-KG5 reference cell (Enli Technology Co., Ltd), and the measurements were performed under

ambient conditions. The EQE measurements for the devices were performed by using EQE measurement system (QE-R, Enli Technology Co., Ltd). All the solar cells were measured under ambient conditions with relative humidity of ~55%, and temperature of 25 ^{o}C.

OLED characterization. The device area was 0.04 cm^2. The luminance was calibrated using a Minolta Chroma Meter CS-100A spectrophotometer (Konica Minolta). The *J–V* characteristics of the OLEDs were measured using a Keithley 2400 source unit.

XRD. XRD patterns were obtained from the samples of perovskite deposited onto the selected substrates using a D2 PHASER X-ray Diffractometer (BRUKER) equipped with a focusing-graded X-ray mirror with a monochromatic CuKα radiation (λ = 1.5406 Å) source. Scans were taken with a 1 mm wide source with X-ray source settings of 30 kV and 10 mA.

AFM. AFM experiments were conducted with a Bruker Dimension Icon AFM (Bruker Nano, Santa Barbara, CA). Silicon probes (Multi75AI-G, Budgetsensors) with a force constant of 3 N/m and a resonance frequency of 75 kHz were used and the images were acquired with 256 × 256 points at a scan rate of 1.0 Hz per line.

UPS. The experiments were performed in a UHV chamber located at the wide range spherical grating monochromator beamline (WR-SGM) of the National Synchrotron Radiation Research Center (NSRRC) in Hsinchu. The measurements were conducted with a SPEC PHOBOIS 150 electron energy analyzer. The binding energy (BE) scale was referenced to the BE of the Au $4f_{7/2}$ core level (84.0 eV) and the Fermi edge of Au.

Kelvin Probe. Work function measurements of PDTON/ITO were also carried out using a UHV Kelvin Probe 2001 system (KP technology Ltd., UK). The pressure in the UHV chamber was 10^{-10} mbar. The work

function values of the samples were referenced to those of hexadecanethiolate SAMs on Au(111) and freshly sputtered gold.[10]

HRTEM. The morphology of the A- and C-PDTON was studied by high resolution transmission electron microscopy (HRTEM) using a Philips/FEI Tecnai 20 G2 S-Twin device. To ensure the removal of acetic acid completely, we prepared TEM sample carefully by dropped the micelle/inverse micelle solution of PDTON on carbon coated copper grid (300 mesh) and heated at close to 100 ^{o}C in vacuum oven for overnight.

HRXPS and NEXAFS spectroscopy. HRXPS and NEXAFS spectroscopy measurements were carried out at the HE-SGM beamline (bending magnet) of the synchrotron storage ring BESSY II in Berlin, Germany, using a custom designed experimental station.[11] Experiments were conducted at room temperature and under UHV conditions. An established experimental procedure was used.[12] The XPS spectra were measured using a Scienta R3000 spectrometer. The X-ray energy was set to 580 eV. The binding energy (BE) scale of the XPS spectra was referenced to the Au $4f_{7/2}$ peak at a BE of 84.0 eV. The acquisition of the NEXAFS spectra was performed at the C K-edge in the partial electron yield mode with a retarding voltage of 150 V. Linear polarized synchrotron light with a polarization factor of ~0.91 was used. The energy resolution was ca. 0.3-0.4 eV, decreasing with increasing photon energy. To monitor the orientational order in the films, the incidence angle of the synchrotron light was varied from 90° (normal incidence; **E**-vector in the surface plane) to 20° (grazing incidence; **E**-vector near the surface normal) in steps of 10–20°. This approach is based on the linear dichroism in X-ray absorption, i.e., the strong dependence of the cross-section of the

resonant photoexcitation process on the orientation of the electric field vector of the linearly polarized light with respect to the molecular orbital of interest.[13]

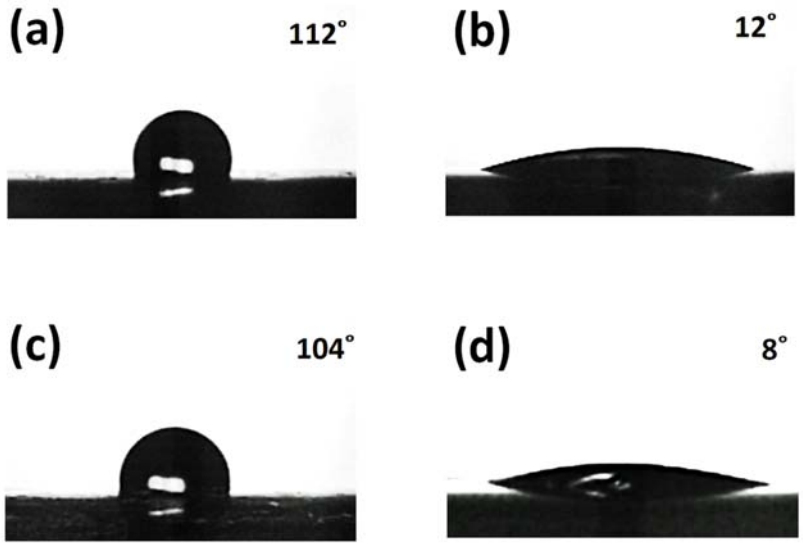

Fig. S6 Reversal change between the two forms of PDTON traced by the static water contact angle. (a) PDTON was dispersed in a proper mixture of acetic acid and ethyl acetate to form A-PDTON, 100 µl solution was dropped on the ITO-coated glass (2×2 cm^2) and annealed at 150 °C for 10 min (standard procedure to form a A-PDTON film; see Methods); the static water contact angle of this film was 112°. (b) the solution prepared in (a) was evaporated with nitrogen flow, the residual, "dry" PDTON was dispersed in a proper mixture of acetic acid and ethyl acetate to form C-PDTON (see Methods), then 100 µl solution was dropped on the ITO glass (2×2 cm^2) and annealed at 150 °C for 10 min; the static water contact angle of this film was 12°. (c) the solution prepared in (b) was evaporated with nitrogen flow, the residual, "dry" PDTON was dispersed in a proper mixture of acetic acid and ethyl acetate to form A-PDTON (see Methods), then 100 µl solution was dropped on the ITO glass (2×2 cm^2) and annealed at 150 °C for 10 min; the static water contact angle of this film was 104°. (d) the solution prepared in (c) was evaporated with nitrogen flow, the residual, "dry" PDTON was dispersed in a proper mixture of acetic acid and ethyl acetate to form C-PDTON (see Methods), then 100 µl solution was dropped on the ITO glass (2×2 cm^2) and annealed at 150 °C for 10 min; the static water contact angle of this film was 8°.

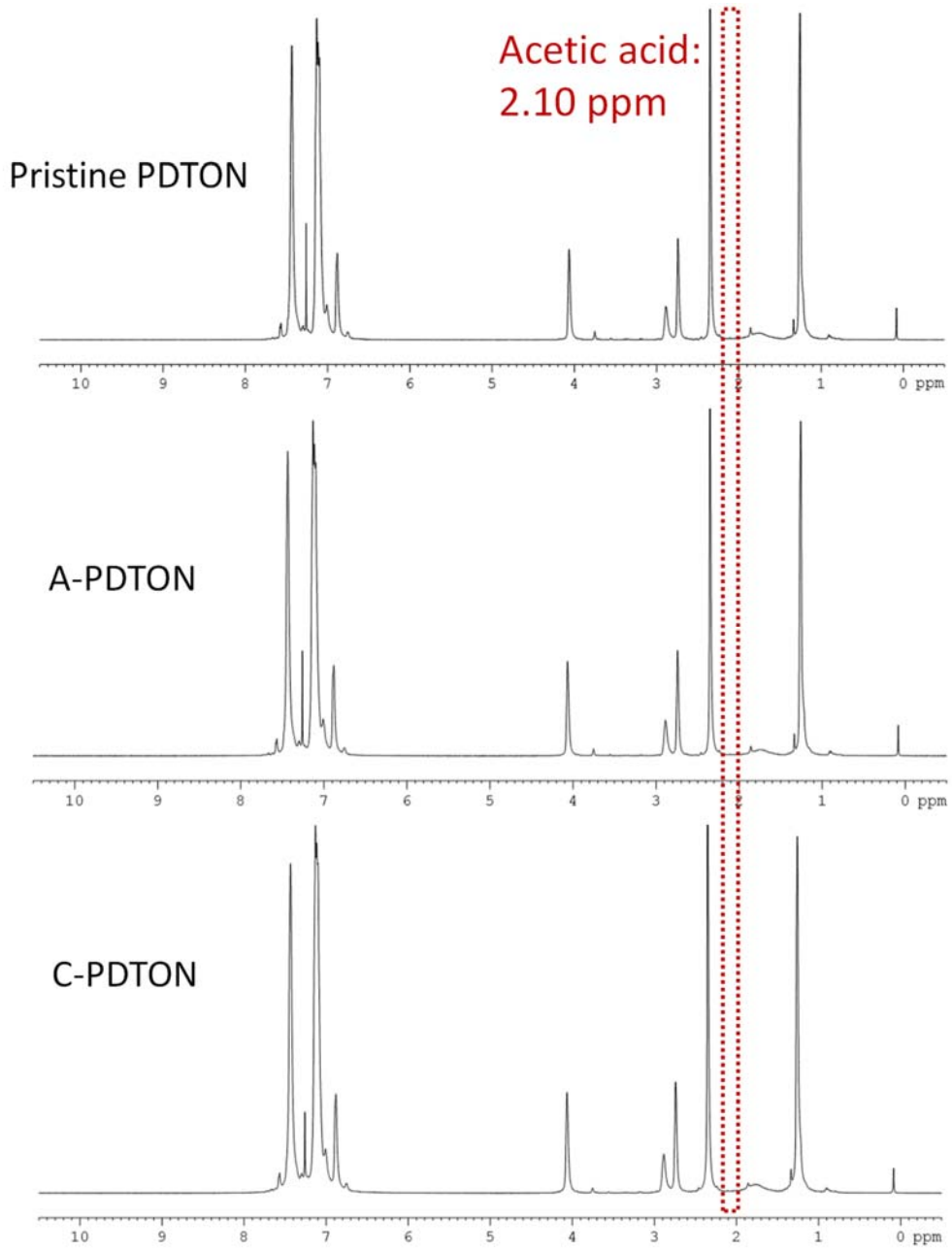

Fig. S7 NMR spectra of pristine PDTON as well as C- and A-PDTON. The pristine PDTON powder was directly dissolved in D_1-chloroform. For sample preparation, the C- and A-PDTON solutions were prepared according to the Method, afterward, the acetic acid and ethyl acetate were removed with nitrogen flow. Thereafter, the samples were completely dried in the 7 ml sample cell, at 150 °C for 10 min, and then dissolved in D_1-chloroform. Note that the annealing mimicked the respective fabrication step always applied during the preparation of the C- and A-PDTON layers. The broad peak at 1.7 ppm and 7.26 ppm corresponds to the water and chloroform (from D_1-chloroform), while the peaks at 1.85 and 3.76 ppm correspond to the tetrahydrofuran.[14]

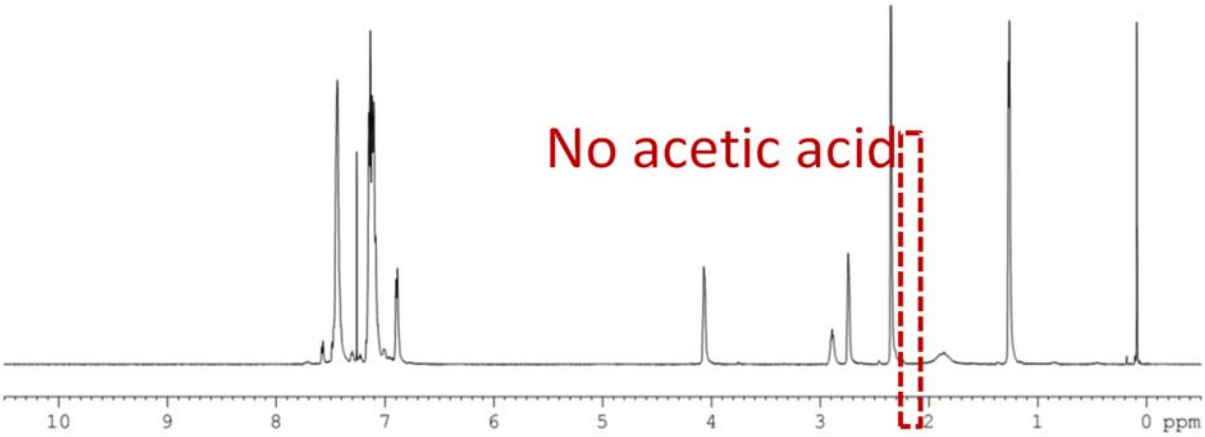

Fig. S8 NMR spectra of PDTON (dissolved in 500 µl acetic acid in ethyl acetate, followed by 100 ºC heating for 30 min in ambient).

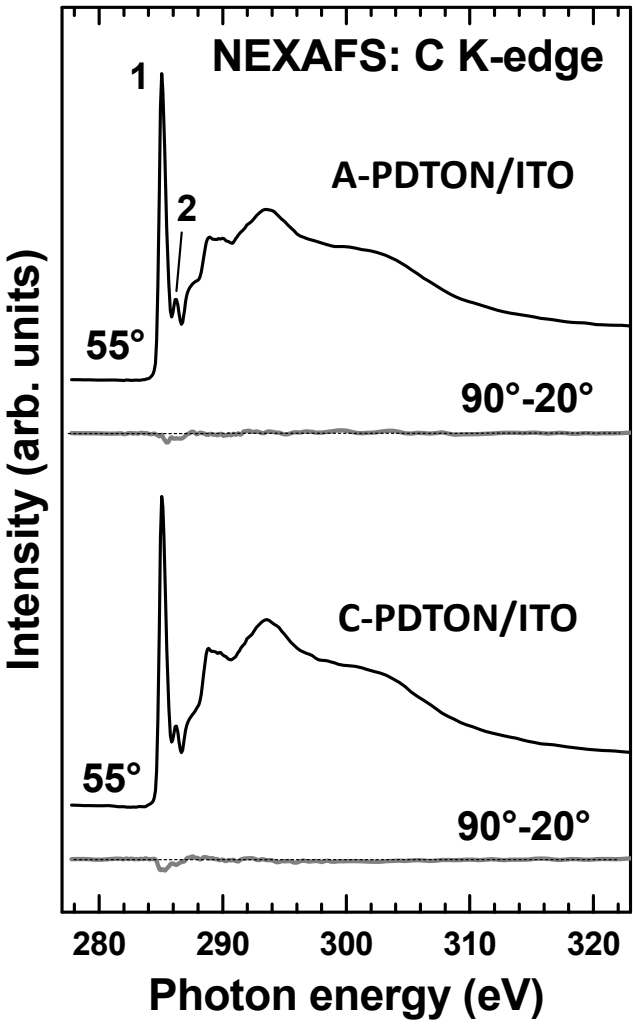

Fig S9 NEXAFS data for the PDTON films. C K-edge NEXAFS spectra of the A- and C-PDTON films deposited onto the ITO substrate acquired at an X-ray incidence angle of 55° (black curves) and the difference between the spectra acquired at X-ray incidence angles of 90° and 20° (gray curves). Most prominent absorption resonances are marked. The 55° spectra are dominated by a strong π_1* orbital of the phenyl rings comprising the backbone and side chains of PDTON (1); they also exhibit a weak feature (2) related to the C1s(C-N)→π* transition, associated with the nitrogen atom in the backbone.[15] A π*(COOH) resonance at ~288.5 eV,[16] corresponding to possible residuals of acetic acid, is not perceptible in the spectra. The horizontal dotted lines correspond to zero.

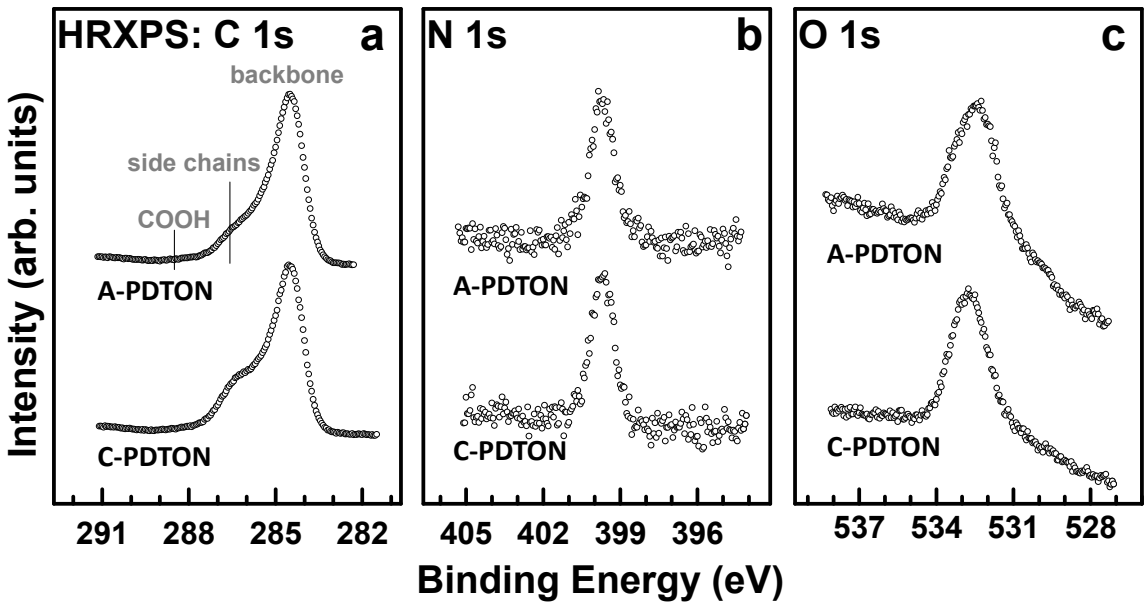

Fig. S10 HRXPS data for the PDTON films. C 1s (a), N 1s (b), and O 1s (c) XPS spectra of the A- and C-PDTON films deposited onto the ITO substrate. The C 1s spectra are the averages over the measurements on three different A- and C-PDTON films; they are normalized to the maximal intensity to simplify the comparison in the spectral weights of the component peaks assigned to the polytriphenylamine backbone (284.5 eV) and the aminoalkyl-containing side chains (~286.3 eV), respectively. Standard position of the COOH signal, which is absent in the given case, is marked. The photon energy is 580 eV. Note that application of XPS to characterization of heterogeneous spherical nanostructures in term of the internal structure is an established approach.[17]

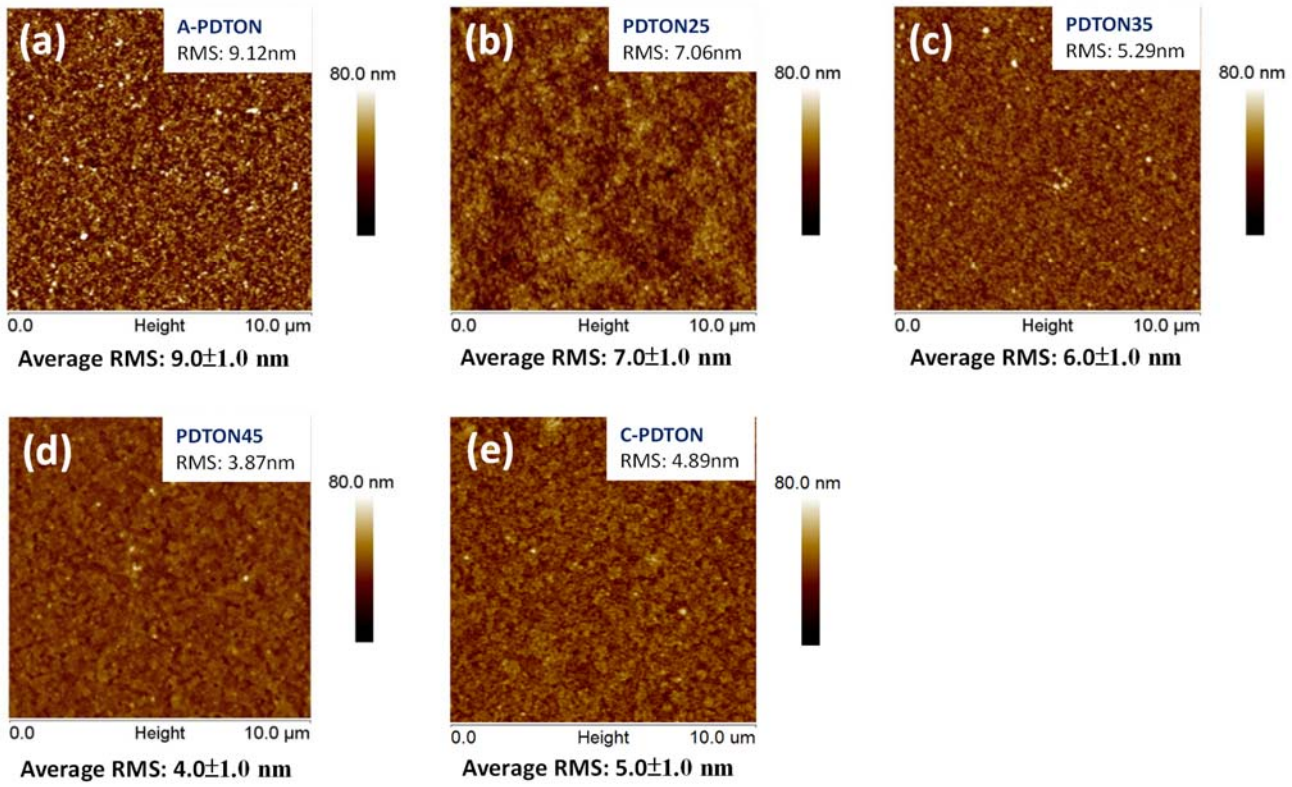

Fig. S11 AFM images of the PDTON films. The PDTON films were prepared from the dispersing solutions of different compositions; the ratio of acetic acid and ethyl acetate in these solutions was varied across the series, set to 55, 45, 35, 25, and 15 mg/ml, respectively. The values of 55 and 15 mg/ml are characteristic of the C- and A-PDTON, respectively, while the other three compositions are intermediate ones. The respective PDTON samples are abbreviated according to the composition ratios.

The PDTON solutions were spin-coated onto the ITO substrates followed by annealing at 150 °C for 10 min. The average RMS of PDTON films were calculated over five individual films.

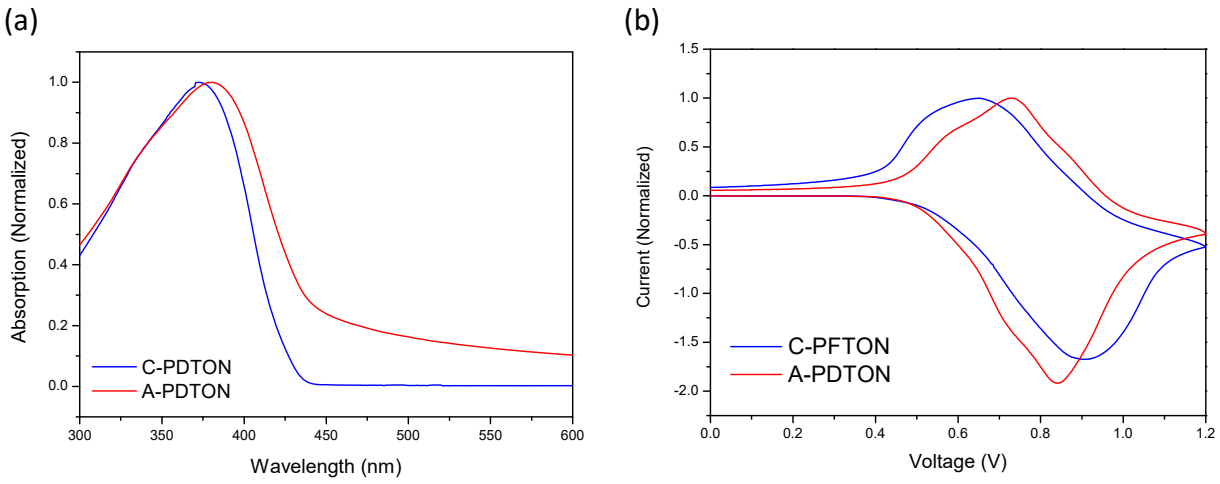

Fig. S12 (a) Absorption spectra of the C- and A-PDTON films on glass and (b) Cyclic voltammograms of these films on ITO substrate. The absorption onset, λ_{onset}, for the C- and A-PDTON is 440 nm and 445 nm, respectively. The bandgaps of the C- and A-PDTON are calculated at 2.80 eV and 2.79 eV, respectively. The CV measurements were performed in acetonitrile solutions containing 0.1 M TBAP under argon atmosphere; the sweep rate was set to 100 mV/s. E_{onset}^{ox} for both C- and A-PDTON is located at approximately 0.6 V; the positions of the HOMO states were calculated by using the empirical formula HOMO = -(4.4 eV + E_{onset}^{ox}) and estimated at -5.0 eV.

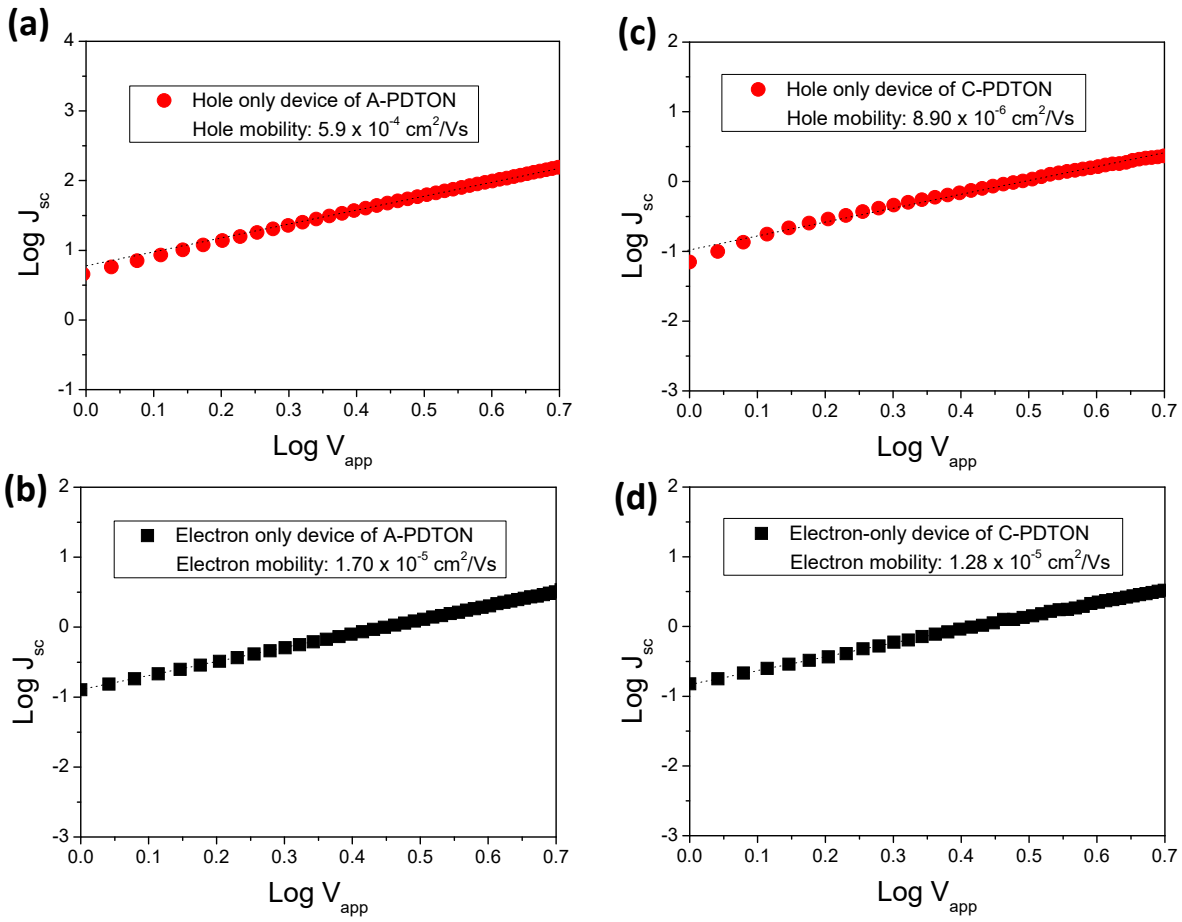

Fig. S13 The results of the SCLC measurements[18] for the A- and C-PDTON films. Experimental Log(J_{sc})–Log(V_{app}) characteristics of (a) the hole-only devices utilizing the A-PDTON films. (b) the electron-only devices utilizing the A-PDTON films. (c) the hole-only devices utilizing the C-PDTON films. (d) the electron-only devices utilizing the C-PDTON films.

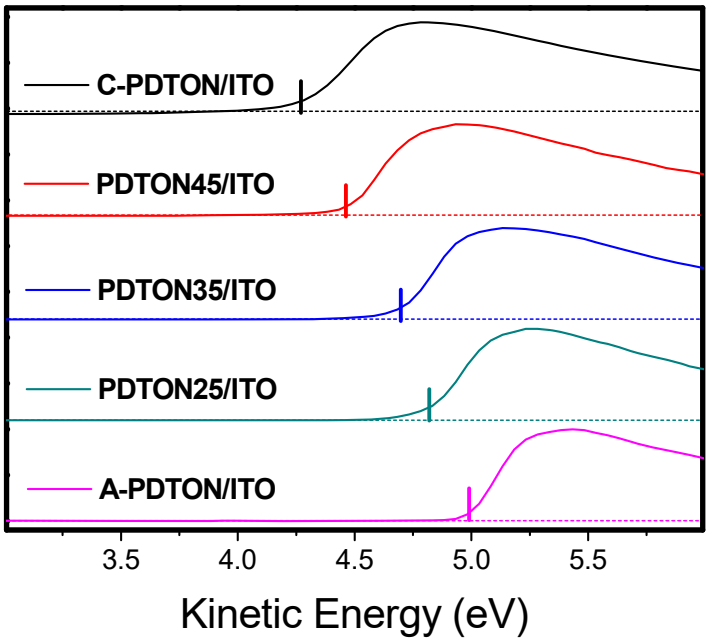

Fig. S14 UPS cutoff spectra of PDTON/ITO. The PDTON films were prepared from the dispersing solution of different compositions; the ratio of acetic acid and ethyl acetate in these solutions was varied across the series, set to 55, 45, 35, 25, and 15 mg/ml, respectively. The values of 55 and 15 mg/ml are characteristic of the C- and A-PDTON, respectively, while the other three compositions are intermediate ones. The respective PDTON samples are abbreviated according to the composition ratios.

The PDTON solutions were spin casted onto the ITO substrates followed by annealing at 150 °C for 10 min. The thickness of the PDTON films was ~7 nm.

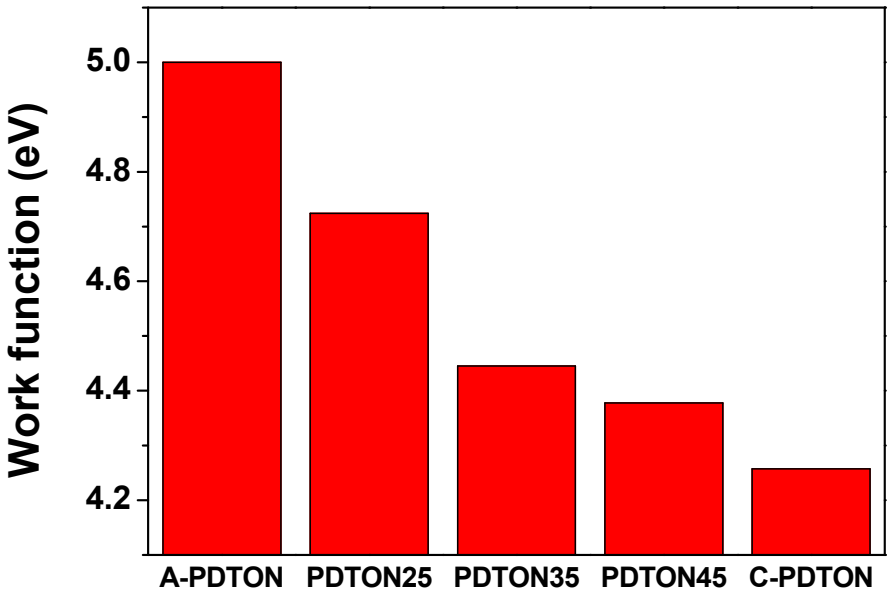

Fig. S15 Work function values of A-PDTON, PDTON25, PDTON35, PDTON45, and C-PDTON on ITO surface measured with Kelvin Probe.

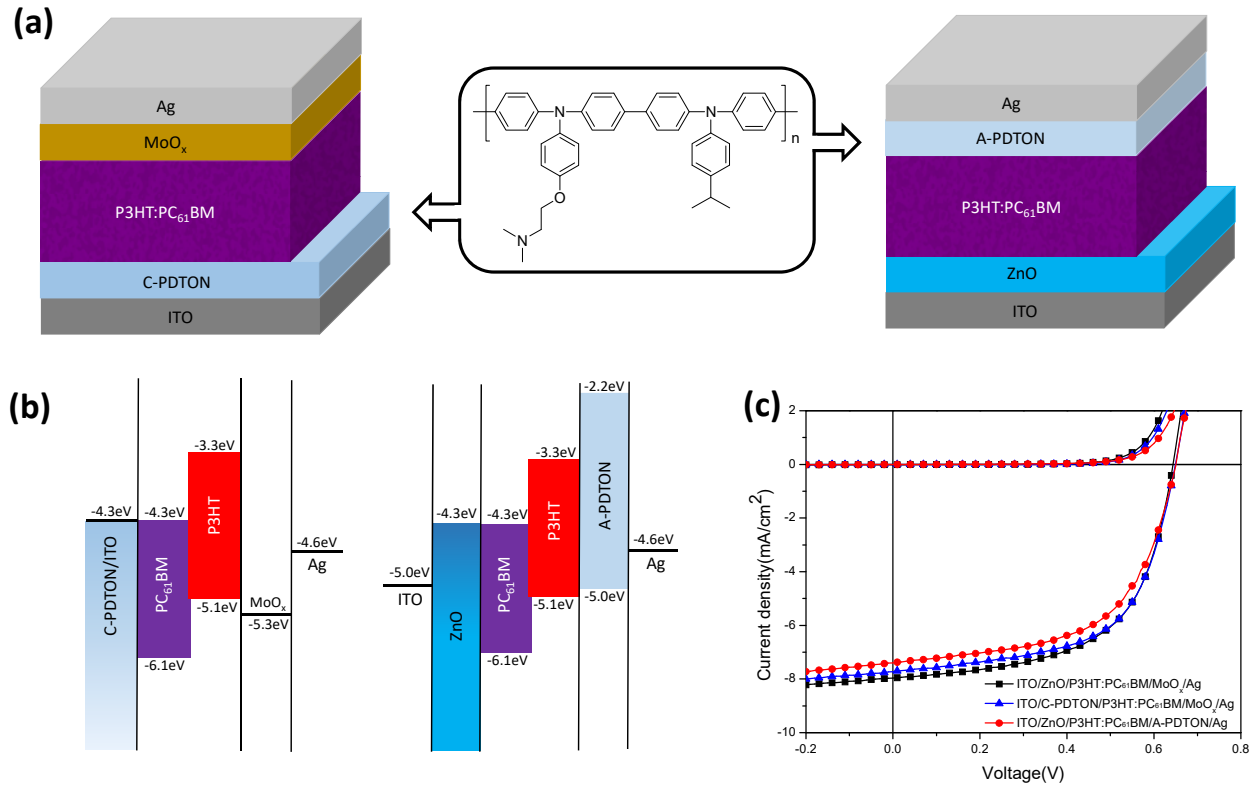

Fig. S16 Structures, energy level alignment diagrams, and *J-V* characteristics of model OSCs. (a) Schematic of the inverted OSCs, whose MoO_x and ZnO layers were substituted by the A- and C-PDTON films, respectively. (b) Energy level alignment diagrams for these OSCs under flat band conditions. **(c)** The *J–V* curves for these OSCs under 100 mW cm^{-2} AM1.5 G illumination.

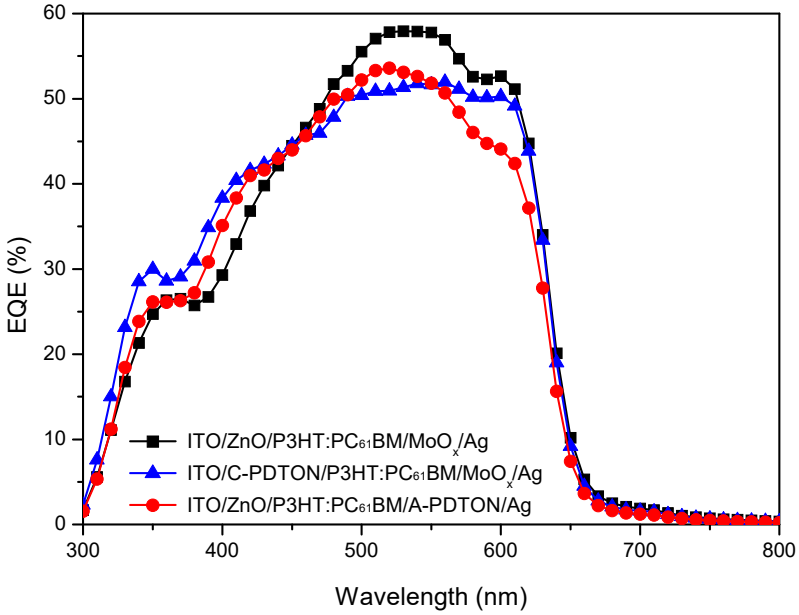

Fig. S17 EQEs of the standard OSC, CBLD, and ABLD. The integrated current density for the standard device (black line and black squares), CBLD (blue line and blue triangles), and ABLD (red line and red circles) were estimated at 7.90 mA/cm^2, 7.57 mA/cm^2, and 7.20 mA/cm^2, respectively, which is consistent with the current densities derived from the *J*–*V* measurements.

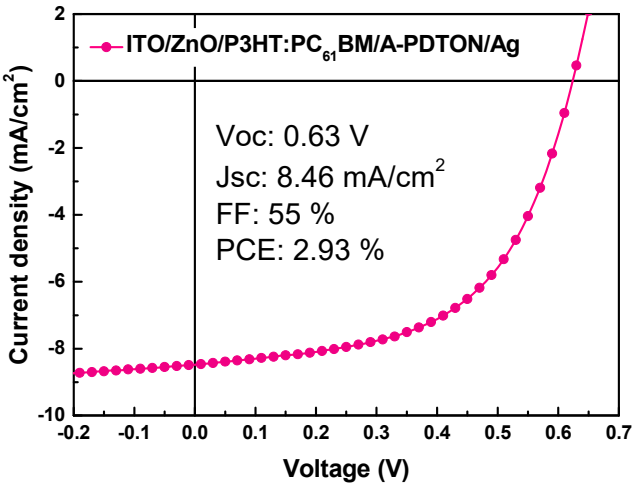

Fig. S18 Current density vs. voltage curve for organic solar cell with configuration of ITO/ZnO/P3HT:$PC_{61}BM$/A-PDTON/Ag, where A-PDTON solution was heated up to 60 °C and spin-coated onto P3HT:$PC_{61}BM$ layer.

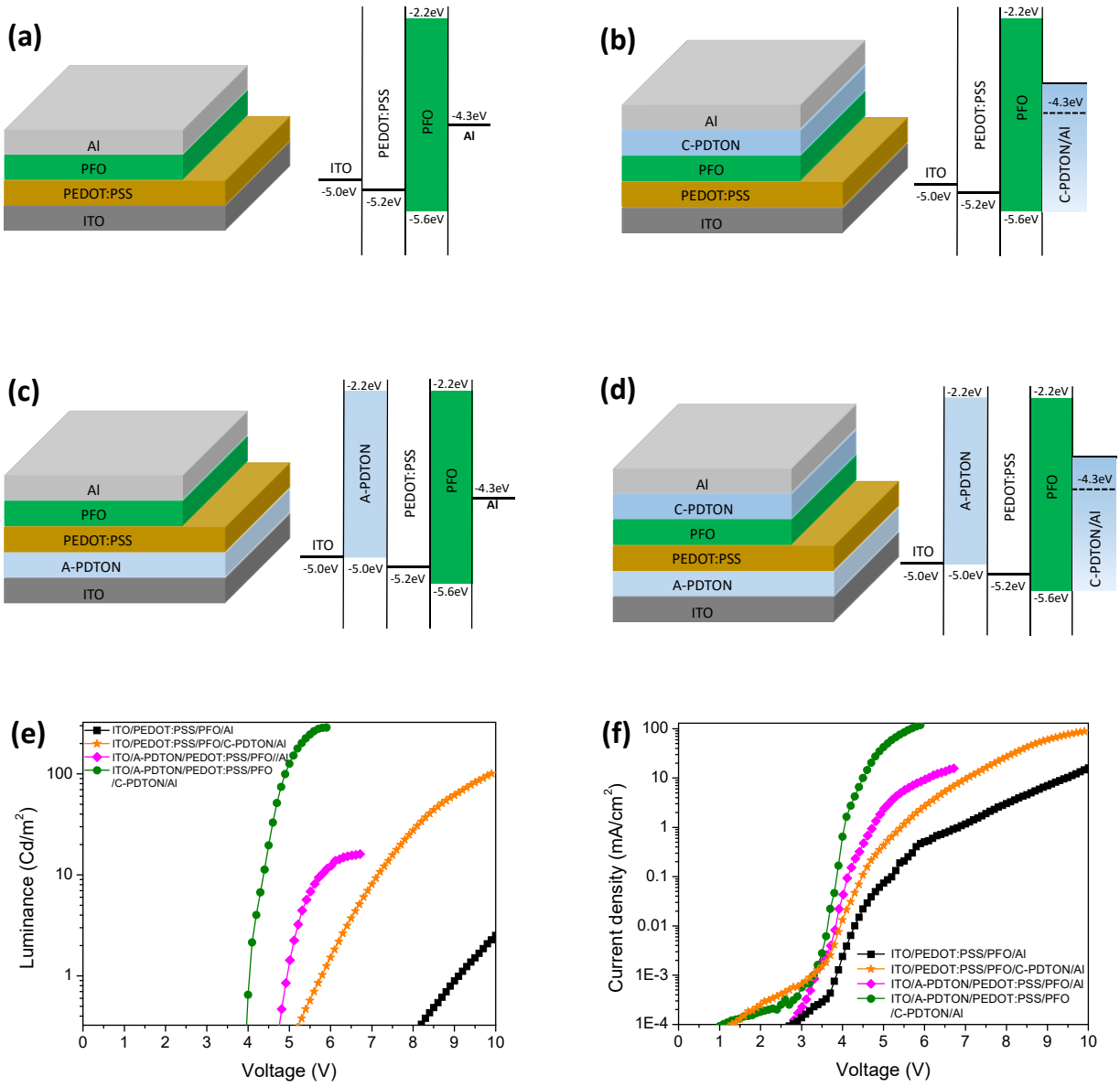

Fig. S19 Structures, energy level alignment diagrams, and basic characteristics of the model OLEDs. (a) Schematic of the ITO/PEDOT:PSS/PFO/Al device and its energy level alignment diagram. (b) Schematic of the ITO/PEDOT:PSS/PFO/C-PDTON/Al device and its energy alignment diagram. (c) Schematic of the ITO/A-PDTON/PEDOT:PSS/PFO/Al device and its energy alignment diagram. (d) Schematic of the ITO/A-PDTON/PEDOT:PSS/PFO/C-PDTON/Al device and its energy alignment diagram. (e) Voltage dependence of the light output. (f) Voltage dependence of the electric current density.

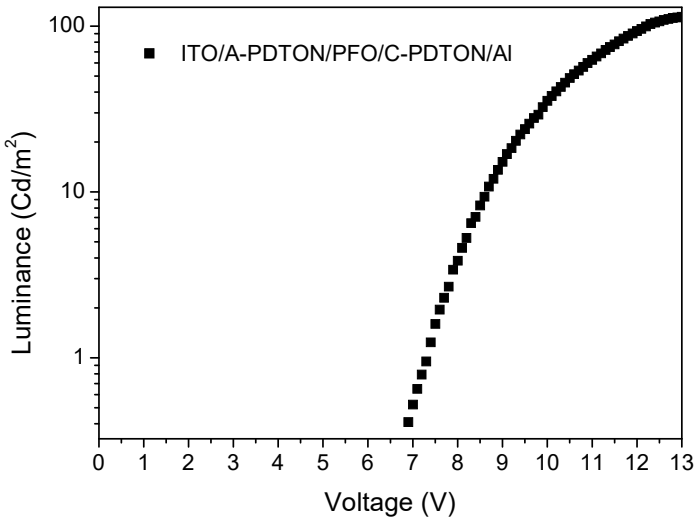

Fig. S20 Voltage dependence of the light output for an OLED device with the ITO/A-PDTON/PFO/C-PDTON/Al configuration.

The given OLED device, using A-PDTON and C-PDTON as anode and cathode buffer layers, exhibits similar luminance (110 Cd/m^2) as the OLED device with configuration of ITO/PEDOT:PSS /PFO/C-PDTON/Al configuration (Fig. 4b). Note that PFO was transferred onto A-PDTON using a transfer technique[7] to prevent dissolution of A-PDTON. The higher turn-on voltage could be attributed to the larger hole injection barrier to PFO for A-PDTON as compared to PEDOT:PSS (HOMO of PDTON: -5.0 eV; work function of PEDOT:PSS: 5.2 eV).[19]

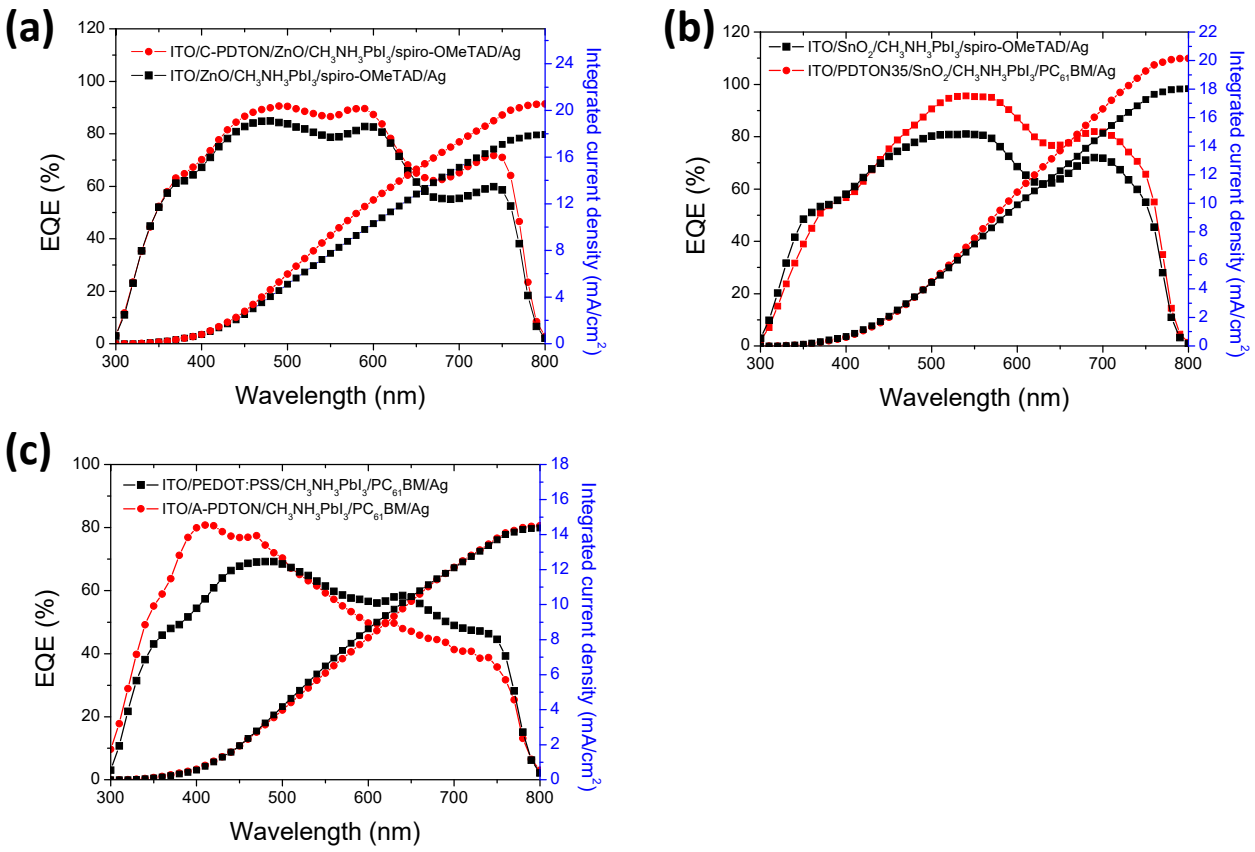

Fig. S21 EQE and integrated current density of model PSCs. (a) ITO/ZnO/perovskite/spiro-OMeTAD/Ag (with an integrated current density of 17.93 mA/cm^2) and ITO/C-PDTON/ZnO/perovskite/spiro-OMeTAD/Ag (with an integrated current density of 20.56 mA/cm^2); (b) ITO/SnO_2/perovskite/spiro-OMeTAD/Ag (with an integrated current density of 18.04 mA/cm^2) and ITO/PDTON35/SnO_2/perovskite/spiro-OMeTAD/Ag (with an integrated current density of 20.17 mA/cm^2); (c) ITO/PEDOT:PSS/perovskite/$PC_{61}BM$/Ag (with an integrated current density of 14.60 mA/cm^2) and ITO/A-PDTON/perovskite/$PC_{61}BM$/Ag (with an integrated current density of 14.38 mA/cm^2). The legends are given in the panels.

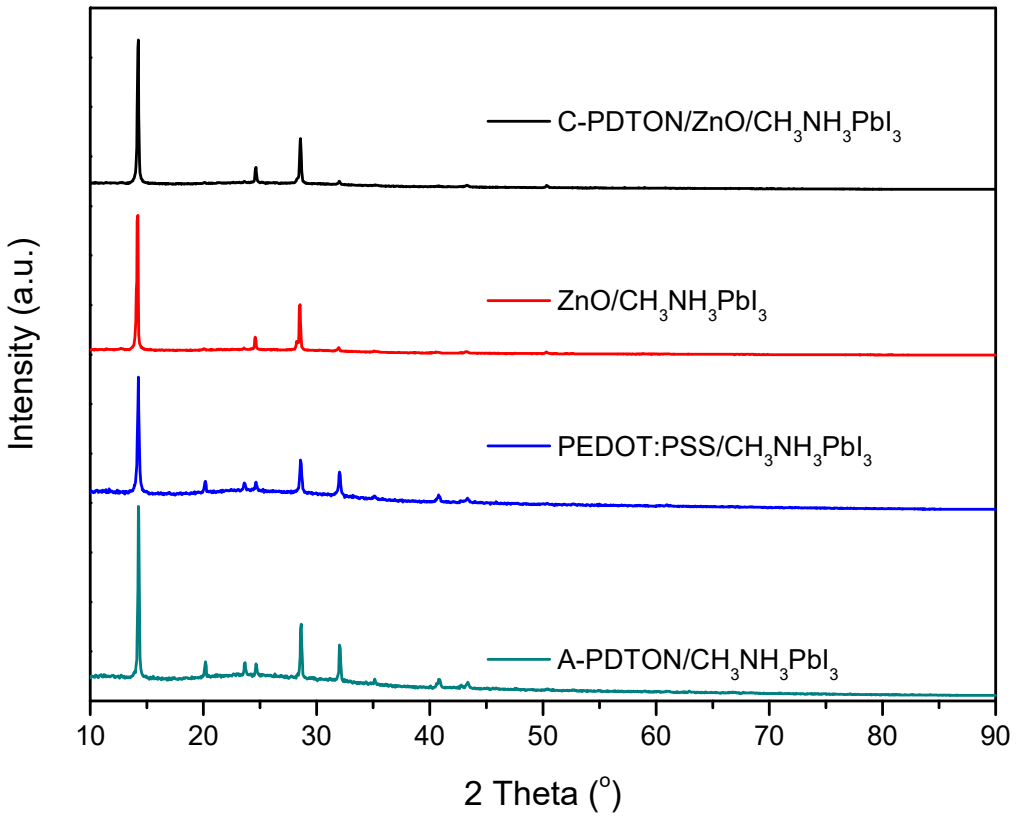

Fig. S22 XRD data for the perovskite films grown on the C-PDTON/ZnO, ZnO, PEDOT:PSS, and A-PDTON substrates.

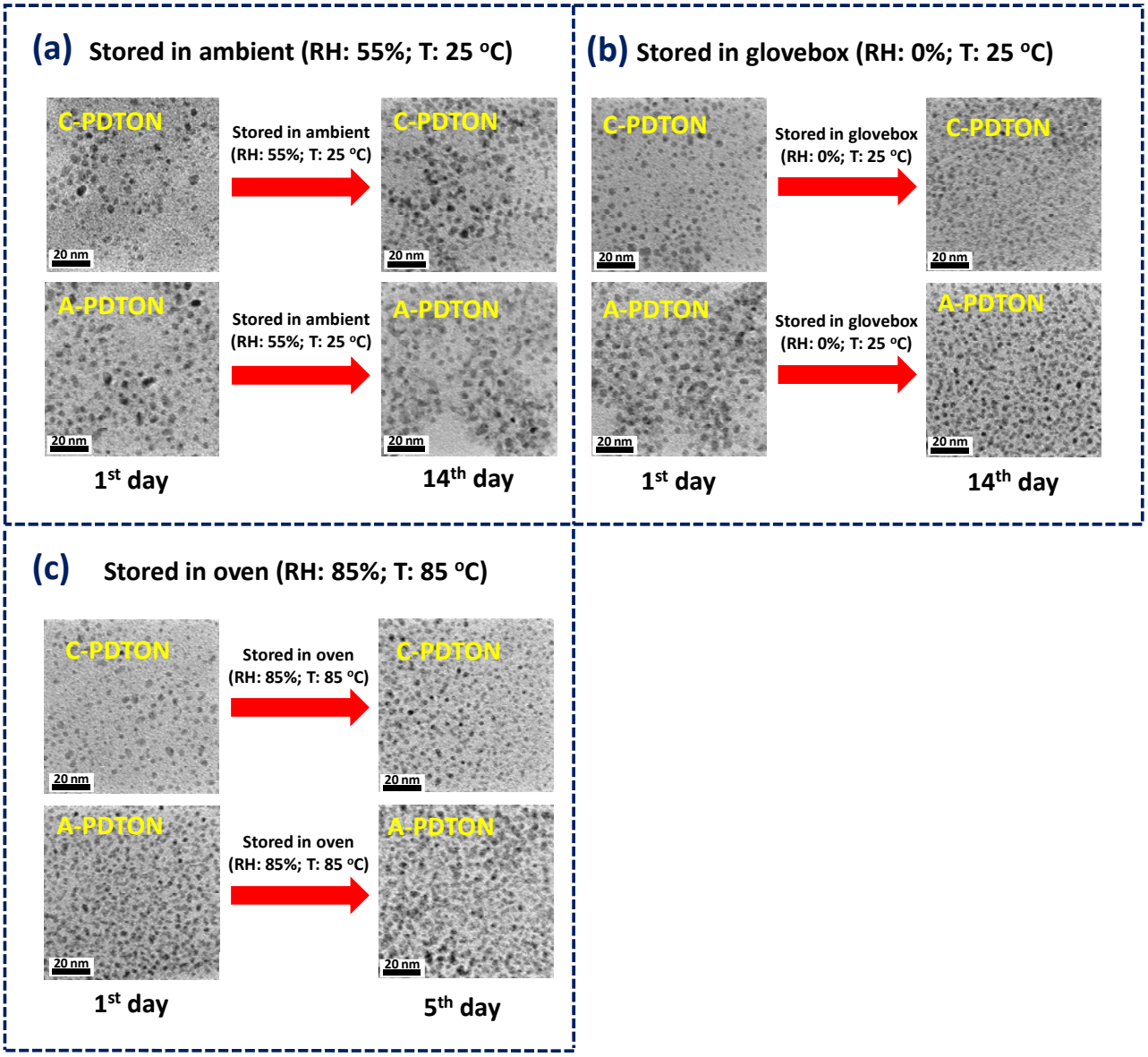

Fig. S23 HRTEM images of C-PDTON and A-PDTON after the preparation (1st day) and after 14 days storage **(a)** under ambient condition (relative humidity (RH): 55%; temperature (T): 25 °C); **(b)** glovebox (relative humidity: 0%; temperature: 25 °C); **(c)** oven (relative humidity: 85%; temperature: 85 °C).

Table S1 Parameters of the solar cells using P3HT:$PC_{61}BM$ active layer and inverted device structure, measured under 100 mW cm^{-2} AM1.5 G illumination.

Structure type	**J_{sc} (mA cm^{-2})**	**V_{oc} (V)**	**FF (%)**	**Average PCE (%)**	**Best PCE (%)**
ITO/ZnO/P3HT:$PC_{61}BM$/MoO_x/Ag	7.7±0.4	0.65±0.01	57±2	2.85±0.20	3.03
ITO/C-PDTON/P3HT:$PC_{61}BM$/MoO_x/Ag	7.4±0.3	0.65±0.01	59±2	2.82±0.09	3.02
ITO/ZnO/P3HT:$PC_{61}BM$/A-PDTON/Ag	7.6±0.5	0.65±0.01	54±3	2.64±0.24	2.77
ITO/C-PDTON/P3HT:$PC_{61}BM$/A-PDTON/Ag	7.3±0.5	0.61±0.02	51±3	2.28±0.17	2.52

FF, fill factor; ITO, indium tin oxide; J_{sc}, short-circuit current density; PCE, power conversion efficiency; V_{oc}, open-circuit voltage; ZnO, zinc oxide; MoO_x, molybdenum oxide.

Each parameter was calculated as an average value over ten devices. The performance of standard device is in accordance with the literature.[20]

Table S2 Summary of the PSC parameters.

Structure type	**J_{sc} (mA cm^{-2})**	**V_{oc} (V)**	**FF (%)**	**Average PCE (%)**
ITO/ZnO/perovskite/spiro-OMeTAD/Ag	18.29±0.48	1.02±0.01	66.56±1.91	12.48±0.03
ITO/C-PDTON/ZnO/perovskite/spiro-OMeTAD/Ag	19.28±1.45	1.01±0.19	73.14±4.11	14.23±0.85
ITO/SnO_2/perovskite/spiro-OMeTAD/Ag	20.18±0.32	1.05±0.02	68.29±2.90	14.44±0.50
ITO/PDTON35/SnO_2/perovskite/spiro-OMeTAD/Ag	21.04±0.21	1.06±0.01	75.33±1.87	16.72±0.32
ITO/PEDOT:PSS/perovskite/$PC_{61}BM$/Ag	16.92±0.89	0.78±0.02	53.39±2.78	7.03±0.41
ITO/A-PDTON/perovskite/$PC_{61}BM$/Ag	14.46±0.32	0.99±0.01	61.84±0.47	8.82±0.10

FF, fill factor; ITO, indium tin oxide; J_{sc}, short-circuit current density; PCE, power conversion efficiency; V_{oc}, open-circuit voltage; each parameter was calculated as an average value over ten devices.

References

1 W. Shi, S. Fan, F. Huang, W. Yang, R. Liu and Y. Cao, *J. Mater. Chem.*, 2006, **16**, 2387-2394.

2 R. Fornasier, P. Scrimin, P. Tecilla and U. Tonellato, *J. Am. Chem. Soc.,* 1989, **111**, 224-229.

3 H. Seyler, D. J. Jones, A. B. Holmes and W. W. H. Wong, *Chem. Commun.,* 2012, **48**, 1598-1600.

4 H. Wu, F. Huang, Y. Mo, W. Yang, D. Wang, J. Peng and Y. Cao, *Adv. Mater.*, 2014, **16**, 1826-1830.

5 D. Liu and T. L. Kelly, *Nat. Photon.,* 2014, **8**, 133-138.

6 C. -H. Chou, W. L. Kwan, Z. Hong, L. -M. Chen and Y. Yang, *Adv. Mater.,* 2011, **23**, 1282-1286.

7 S. H. Kim, J. Yoon, S. O. Yun, Y. Hwang, H. S. Jang and H. C. Ko, *Adv. Funct. Mater.,* 2013, **23**, 1375-1382.

8 W. Ke, G. Fang, Q. Liu, L. Xiong, P. Qin, H. Tao, J. Wang, H. Lei, B. Li, J. Wan, G. Yang and Y. Yan, *J. Am. Chem. Soc.* 2015, **137**, 6730-6733.

9 A. Guerrero, J. You, C. Aranda, Y. S. Kang, G. Garcia-Belmonte, H. Zhou, J. Bisquert and Y. Yang, *ACS Nano,* 2016, **10**, 218-224.

10 T. Abu-Husein, S. Schuster, D. A. Egger, M. Kind, T. Santowski, A. Wiesner, R. Chiechi, E. Zojer, A. Terfort and M. Zharnikov, *Adv. Func. Mater.* 2015, **25**, 3943-3957.

11 A. Nefedov and C. Wöll, *Advanced applications of NEXAFS spectroscopy for functionalized surfaces*, Surface Science Techniques, Springer-Verlag, Berlin, Heidelberg, 2013.

12 C. Musumeci, G. Zappalà, N. Martsinovich, E. Orgiu, S. Schuster, S. Quici, M. Zharnikov, A. Troisi, A. Licciardello and P. Samorì, *Adv. Mater.,* 2014, **26**, 1688-1693.

13 J. Stöhr, *NEXAFS spectroscopy*, Springer-Verlag, Berlin, Heidelberg, 1992.

14 G. R. Fulmer, *Organometallics,* 2010, **29**, 2176-2179.

15 B. Watts, S. Swaraj, D. Nordlund, J. Lüning, and H. Ade1, *J. Chem. Phys.,* 2011, **134**, 024702.

16 I. Cebula, H. Lu, M. Zharnikov and M. Buck, *Chem. Sci.,* 2013, **4**, 4455–4464.

17 B. Pal, S. Mukherjee and D. D. Sarma, *J. Electron Spectr. Relat. Phenom.,* 2015, **200**, 332–339.

18 J. You, L. Dou, K. Yoshimura, T. Kato, K. Ohya, T. Moriarty, K. Emery, C.-C. Chen, J. Gao, G. Li, Y. Yang, *Nat. Commun.*, 2013, **4**, 1446.

19 Y. C. Chao, Y. C. Lin, M. Z. Dai, H. W. Zan, H. F. Meng, *Appl. Phys. Lett.,* 2009, **95**, 203305.

20 F. Liu, D. Chen, C. Wang, K. Luo, W. Gu, A. L. Briseno, J. W. P. Hsu, T. P. Russell, *ACS Appl. Mater. Interfaces*, 2014, **6**, 19876-19887.